Analytical and numerical study concerning the behaviour of single-sided bonded patch repairs

Adriana SANDU*[1], Marin SANDU[1], Loredana TERZEA[1], Gheorghi OPATCHI[1]

*Corresponding author
*[1]"POLITEHNICA" University of Bucharest
Splaiul Independenței 313, 060042, Bucharest, Romania
agsandu@yahoo.com

DOI: 10.13111/2066-8201.2011.3.2.8

Abstract: *Adhesive bonded joints are used in the assembling of structural parts, especially of those which are made from dissimilar materials. Lightweight fibre reinforced polymer composites and other adhesive bonded components represent a major proportion of a modern aircraft. Bonded patch repair technology has been widely used to repair cracked thin-walled structures to extend their service life, because a correctly executed repair significantly enhances the structural performance.*
In practice, the single-sided bonded patch repair is the most used because a good solution like the double-sided repair may not be an option if the access to the structure is only available from one side. This paper presents a relatively simple and effective design procedure for the single strapped bonded joints. Also, the influence of various geometrical parameters of the joint is evaluated. The analytical development is validated based on nonlinear finite element analyses.

Key Words: *analytical and numerical study, single-sided patch repairs, design procedure*

1. INTRODUCTION

The most important loadings of an aircraft structure are induced by the fatigue cycles due to various fluctuant stresses induced first of all by the cabin pressurizations and in the take-off and landing stages. In these conditions it is inherent that crack, impact, and corrosion flaws develop throughout the substructure elements and the external cover of the aircraft. The repair technique by using bonded composite doublers offers maintenance facilities to safely extend the aircrafts lifetime [1]. During the last decades, adhesive bonding has been widely used to construct and repair advanced structures, especially in the aircraft and automotive fabrication. The main advantage is the possibility to join parts from dissimilar materials as polymers, polymeric composites, aluminium, magnesium or other metal alloys. Bonded structures have been shown to be far more fatigue resistant than equivalent mechanically fastened structures.

They are also low-priced and lighter due to the absence of fasteners and easier inspected by using non-destructive techniques. The mechanical strength of adhesive bonded joint is strongly dependent on the adhesive properties, but the configuration of the joint and the bonding technique are also important. A correct evaluation of the operating behaviour of adhesively bonded joints is necessary to ensure the efficiency, safety and reliability of this kind of assembling [2]-[8]. In many aircraft repairs the most used practical joint configuration is the single-strap joint because the access is available only from the external side of the structure. Usually, to repair a locally damaged structure, the patch is used to bridge a crack or to cover over a hole. One of the objectives of paper [7] was to deny the statement that a single-strapped joint is less efficient than a single-lap joint.

This task was accomplished through a detailed analytical and numerical investigation of the joint parameters that govern the peak stresses in the adhesive.

If the outer adherends and the inner adherend (strap or patch) have the same tensile and bending stiffness, the joint is so-called balanced. In paper [7] the deformations of a typical unbalanced single-strapped joint were determined analytically and subsequently used to calculate the bending moments and the shear forces at the two ends of the overlap, that affect the peak stresses in the adhesive. In the case of a balanced single-strapped joint, closed-form solutions were obtained, but for an unbalanced joint the two differential equations are coupled and the solution can only be obtained numerically.

It must be pointed out that thermally induced stresses are added to the stresses caused by a mechanical load. They can therefore lead to early failure in certain cases even if their amplitude is small.

Consequently, estimating these stresses is an important issue which is already discussed in the literature [9], [10]. In the present paper only the effect of tensile forces acting on single-strapped bonded joints with various configurations of the adherends ends in the overlap zone is analysed.

2. PRELIMINARY DESIGN OF SINGLE-SIDED BONDED JOINTS BASED ON ANALYTICAL RELATIONS

In practical engineering design, simple and accurate analytical solutions are very useful because they can provide a relatively fast preliminary estimation of the structural performances. Subsequent finite element analyses or experimental investigations are not always necessary.

A pre-dimensioning algorithm will be presented by using the calculus relations deduced in paper [7] for balanced single-strap joints with thin adhesive layer. The relations from the cited paper will be rewritten in a more convenient form for the design purposes. Three configurations of single-sided adhesive bonded repairs, with adherends of constant thickness (Fig. 1, a), with tapered adherends (Fig. 1, b) and with stepped adherends (Fig. 1, c) will be analyzed based on the same calculus scheme (Fig. 1, d).

A preliminary evaluation of the load capacity P (axial load per unit width) can be made as to accomplish the strength conditions in some locations of the joint.

Allowable values are required for: a) combined tensile and bending maximum stress in the outer adherend, near the outer end of the overlap (zone 1), b) combined tensile and bending maximum stress in the inner adherend (strap), at middle and near the inner end of the overlap (zone 3), c) maximum equivalent stresses in adhesive (zone 2), at the adhesive layer ends.

The considered geometry (Fig. 1, a) permits to analyse different cases when the overlap (L_2) and the gap ($2L_3$) are small, mean or large. Figure 2 shows the typical deformed shape in the case of a single-strapped joint.

Establishing the allowed load will be a relatively difficult task because the dependence between the applied load and the stress state in the joint is nonlinear. Due to symmetry, the discussion that follows refers to a half of the single-strapped joint, on which local axes were considered for each zone (Fig. 1, d).

The adherends were considered as cylindrically bended plates with bending stiffnesses:

$$D_k = \frac{E\, h_k^3}{12\,(1-\nu^2)} \qquad (k = 1,\ 2,\ 3) \tag{1}$$

where $h_1 = h_3 = h$ is the thickness of adherends which are made from the same material having the elastic modulus E and the Poisson's ratio ν.

The adhesive layer has a very small thickness h_a ($h_a << h$). Based on the assumption that the overlap (zone 2) work as a monolithic part, the thickness h_2 (Fig. 1,d) will be considered as $h_2 = h_1 + h_3 + h_a$ in case of variant with right adherends (Fig. 1,a), and as $h_2 = h_1 + h_4 + h_a$ when the adherends ends are tapered (Fig. 1,b) or stepped (Fig. 1,c).

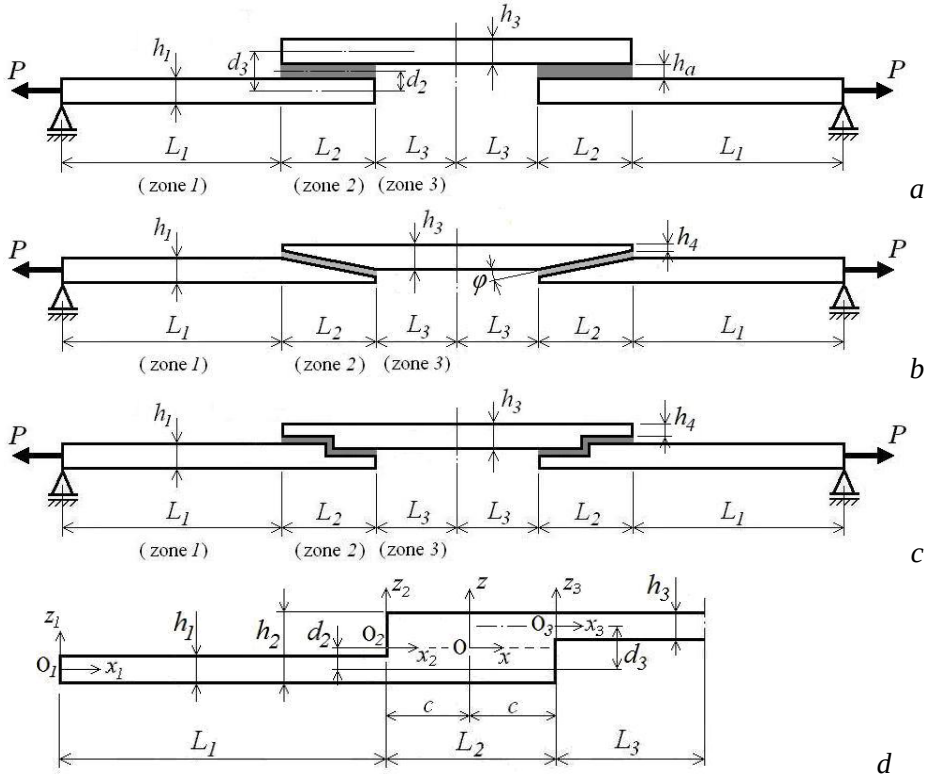


Fig. 1 – Geometries of bonded patch repairs: a) with right adherends, b) with tapered adherends, c) with stepped adherends, d) the simplified calculus scheme



Fig. 2 – Deformed shape in the case of a single strapped joint in tension

Only the final calculus relations that are used to determine the maximum deflection w_{max} at the middle of the strap, the maximum bending stresses in the adherends and the distribution of the shear and peel stresses along the adhesive layer will be presented here.

The main purpose of developing an analytical solution was the evaluation of the bending moments and shear forces at the inner and outer ends of the overlap (M_i , V_i and M_o ,V_o). Their expressions, in a condensed form, are:

$$M_i = -\frac{P}{N_3}\left[\left(d_3 - d_2\right)N_2 + \frac{d_2}{\cosh\left(\beta_2 L_2\right)}\right] \tag{2}$$

$$M_o = \frac{P \cdot \tanh(\beta_1 L_1)}{N_3}\left[N_1 + d_2\left(\frac{\beta_2}{\beta_1}\tanh(\beta_2 L_2) + \frac{\beta_3}{\beta_1}\tanh(\beta_3 L_3)\right)\right] \tag{3}$$

$$V_i = -\beta_3 M_i \tanh(\beta_3 L_3), \qquad V_o = \beta_1 M_o \frac{1}{\tanh(\beta_1 L_1)} \tag{4}$$

where

$$\beta_k = \sqrt{\frac{P}{D_k}} \qquad (k = 1,\ 2,\ 3), \tag{5}$$

$$N_1 = \frac{\beta_3}{\beta_1} \cdot \frac{\tanh(\beta_3 L_3)}{\cosh(\beta_2 L_2)} \cdot (d_3 - d_2) \tag{6}$$

$$N_2 = 1 + \frac{\beta_2}{\beta_1} \cdot \tanh(\beta_1 L_1) \cdot \tanh(\beta_2 L_2) \tag{7}$$

$$N_3 = N_2 + \beta_3 \cdot \tanh(\beta_3 L_3) \cdot \left(\frac{\tanh(\beta_1 L_1)}{\beta_1} + \frac{\tanh(\beta_2 L_2)}{\beta_2}\right) \tag{8}$$

To calculate the maximum deflection will be used the formula

$$w_{\max} = -\frac{1}{N_3 \cosh(\beta_3 L_3)} \cdot \left[(d_3 - d_2) + \frac{d_2}{\cosh(\beta_2 L_2)}\right] + d_3 \tag{9}$$

The distribution of the shear and peel stresses (τ and σ) in the adhesive, along the overlap (where $-c \le x \le c$ and $c = L_2 / 2$), can be estimated by using the expressions [6], [7]

$$\tau = C_0 + C_1 \cosh(\lambda x) + C_2 \sinh(\lambda x) \tag{10}$$

$$\begin{aligned}\sigma = {} & C_3 \cosh(\xi x)\cos(\xi x) + C_4 \cosh(\xi x)\sin(\xi x) + \\ & + C_5 \sinh(\xi x)\cos(\xi x) + C_6 \sinh h(\xi x)\sin(\xi x)\end{aligned} \tag{11}$$

where

$$\lambda = \sqrt{\frac{G_a}{h_a} \cdot \left(\frac{2}{E\,h} + \frac{h(h + h_a)}{2D}\right)} \qquad \xi = \sqrt[4]{\frac{E_a}{2\,h_a\,D}} \tag{12}$$

as E_a , G_a are the tensile and the shear modules of the adhesive and $D = D_1 = D_3$.

The values of constants C_i (i = 0, 1,…, 6) will be calculated by formulas

$$C_0 = \frac{P}{2c} - \frac{G_a}{2\,c\,\lambda^2\,h_a} \cdot \left[\frac{2P}{Eh} + \frac{h}{2D} \cdot (M_o - M_i)\right] \tag{13}$$

$$C_1 = \frac{G_a}{\lambda\,h_a \sinh(\lambda c)} \cdot \left[\frac{P}{Eh} + \frac{h}{4D} \cdot (M_o - M_i)\right] \tag{14}$$

$$C_2 = -\frac{G_a}{\lambda\,h_a \cosh(\lambda c)} \cdot \frac{h}{4D}(M_o + M_i) \tag{15}$$

$$C_3 = \frac{E_a}{4\,D\;h_a\;N_4}\left[\xi\left(H_{SC} - H_{CS}\right)\left(M_o - M_i\right) + H_{CC}\left(V_o + V_i\right)\right] \tag{16}$$

$$C_4 = \frac{E_a}{4\,D\;h_a\;N_5}\left[\xi\left(H_{CC} + H_{SS}\right)\left(M_o + M_i\right) + H_{CS}\left(V_o - V_i\right)\right] \tag{17}$$

$$C_5 = \frac{E_a}{4\,D\;h_a\;N_5}\left[\xi\left(H_{CC} - H_{SS}\right)\left(M_o + M_i\right) + H_{SC}\left(V_o - V_i\right)\right] \tag{18}$$

$$C_6 = \frac{E_a}{4\,D\;h_a\;N_4}\left[\xi\left(H_{SC} + H_{CS}\right)\left(M_o - M_i\right) + H_{SS}\left(V_o + V_i\right)\right] \tag{19}$$

where

$$N_4 = \xi^3\left(\cos\left(\xi c\right)\sin\left(\xi c\right) + \cosh\left(\xi c\right)\sinh\left(\xi c\right)\right) \tag{20}$$

$$N_5 = \xi^3\left(\cos\left(\xi c\right)\sin\left(\xi c\right) - \cosh\left(\xi c\right)\sinh\left(\xi c\right)\right) \tag{21}$$

$$H_{CC} = \cosh\left(\xi c\right)\,\cos\left(\xi c\right)\;, \qquad H_{SS} = \sinh\left(\xi c\right)\sin\left(\xi c\right) \tag{22}$$

$$H_{CS} = \cosh\left(\xi c\right)\,\sin\left(\xi c\right)\;, \qquad H_{SC} = \sinh\left(\xi c\right)\cos\left(\xi c\right) \tag{23}$$

Starting from the values of shear and peel stresses in the critical point of the adhesive, an equivalent stress can be calculated based on the von Mises's criterion

$$\sigma_{eq} = \sqrt{\sigma^2 + 3\,\tau^2} \tag{24}$$

Following the design guide [11], the Hill's failure criterion will be applied to determine the maximum load that does not induce damages in the adhesive.

The actual stress state is allowable in a point of the adhesive layer if the condition

$$\chi = \left(\frac{\sigma}{\sigma_{fa}}\right)^2 + \left(\frac{\tau}{\tau_{fa}}\right)^2 \le 1 \tag{25}$$

is accomplished (σ_{fa}, τ_{fa} are tensile and shear ultimate strengths of the adhesive).

Also, the strength condition for the adherends (zones 1 and 3) can be written as

$$\sigma_{\max,ad} = \max\left(\sigma_{\max,I}\,,\;\sigma_{\max,III}\right) \le \sigma_a \tag{26}$$

where

$$\sigma_{\max,I} = \frac{P}{h} + \frac{6\,M_o}{h^2}\,; \qquad \sigma_{\max,III} = \frac{P}{h} + \frac{6\,\left|M_i\right|}{h^2} \tag{27}$$

and σ_a is the allowable stress in the material of the adherends.

In the case of tapered adherends (Fig. 1, b) it is necessary to make a correction into relations (16)-(19) i.e. the binomials $(V_o \pm V_i)$ must be replaced with $(V_o \pm V_i)\,\cos\varphi$.

In fact, in the majority of practical cases $\varphi < 8^o$ and the correction is not necessary because $\cos\varphi \approx 1$.

3. COMPARISON OF ANALYTICAL AND NUMERICAL RESULTS

Results obtained using the above presented relations will be compared with numerical ones, established by linear and nonlinear finite element analyses (LFEAs and NFEAs). The numerical results which will be discussed in this section were obtained by NFEAs performed by using the COSMOS/M Finite Element System [12]. Each nonlinear analyse was developed by applying the load in 100 steps. If the final loading is too large and induces stresses of unacceptable values in adhesive and/or in the adherends, it is possible to identify the load capacity of the joint in a relatively simple manner: the load capacity is the maximum force which corresponds to a loading step where all strength conditions are accomplished. Plane strain state and four node quadrilateral finite elements were used in the generation of numerical models. In order to validate the analytical model and to identify its limits of applicability, some numerical sets of joint geometric parameters were considered. In all cases was used the structural adhesive AV 119 (also known as Araldite® 2007) which has the following elastic and strength characteristics: $E_a = 3000$ MPa, $\nu_a = 0.35$, $\sigma_{fa} = 70$ MPa, $\tau_{fa} = 47$ MPa. The shear modulus was deduced based on the assumption that the adhesive is an isotropic material, i.e. $G_a = 0.5 \cdot E_a /(1 + \nu_a) = 1110$ MPa. The first case which will be discussed refers to a balanced single-strapped joint with right adherends (Fig. 1, a) made from aluminium alloy having the elastic modulus E = 70000 MPa, the Poisson's ratio ν = 0.33 and the allowable stress $\sigma_a = 180$ MPa. The applied axial load (per unit width), P = 145 N/mm, induces a nominal tensile stress σ_n=50 MPa into the adherends. Dimensional parameters which were taken into account are: $L_1 = 80$ mm, $L_2 = 40$ mm, $L_3 = 10$ mm, $h = h_1 = h_3 = 2.9$ mm, $h_a =$ and 0.2 mm. The same main parameters were maintained for a joint with tapered adherends (Fig. 1, b) with $h_4 = 0.5$ mm and for a joint with stepped adherends (Fig. 1, c) with $h_4 = h_3 / 2$. In these conditions, the above discussed correction for the case of tapered adherends is not necessary, because the tapering angle is small, $\varphi = \arctan\left[(h_3 - h_4) / L_2\right] = 3.43^o < 8^o$. The values presented in table 1 emphasize a good agreement between analytical and nonlinear elastic finite element analysis (NFEA) results. The linear elastic finite element analysis (LFEA) predicts correctly only the maximum equivalent stress in the outer adherend. Consequently, this kind of joint must be evaluated based on nonlinear analytical and numerical models.

Table 1 - Comparison between analytical and numerical results

Variant	Calculus method	Maximum equivalent stresses in adherends [MPa]		Stresses at the inner ends of adhesive layers[MPa]			Maximum deflection [mm]
		Inner adherend	Outer adherend	σ_{max}	τ_{max}	$\sigma_{eq,max}$	
right adherends	Analytic	237	113	58	38	87.7	1.37
	NFEA	240	135	59.7	39.5	90.8	1.54
	LFEA	395	114	111	66	159	5.46
tapered adherends	Analytic	88.7	67.3	12.0	16.8	31.5	0.342
	NFEA	91.1	72.0	13.5	14.6	28.7	0.376
	LFEA	130	69.6	20.3	21.3	42.1	1.77
stepped adherends	Analytic	146	86.5	29.7	25	52.5	0.887
	NFEA	152.8	96.5	39.4	22	51.4	0.79
	LFEA	239.7	84.5	66.4	35.1	84.4	3.04

The main conclusion is that by tapering the adherends edges a spectacular diminution of maximum stresses in all components of the joint was obtained. In fact this is the effect of the reduction of the joint eccentricity (d_3) that is of 3.1 mm, 1.65 mm and 0.7 mm in the cases of right, stepped and tapered adherends, respectively.The best and the worst variants will be compared based on results obtained by NFEAs. The diagrams from figure 3, which present the distribution of shear and peel stresses in the adhesive in the case of right adherends, emphasize a strong stress concentration at the inner ends of the overlap (at the interface with the strap) and a less loaded portion (in the vicinity of the overlap middle).

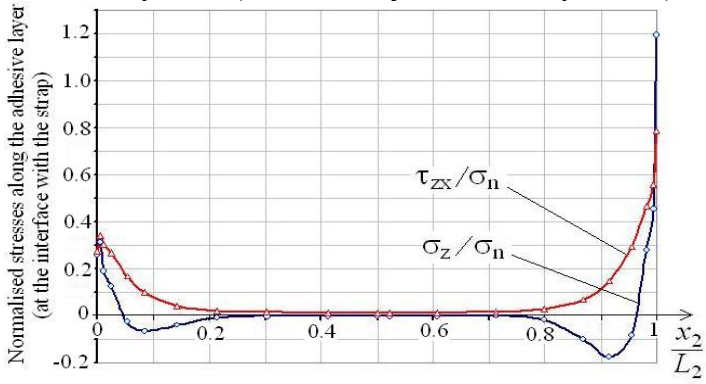


Fig. 3 - Distribution of shear and peel stresses along the adhesive layer in the case of a single-strapped joint with right adherends at the interface with the strap

The stresses were normalised by dividing them with the nominal tensile stress in the outer adherends $\sigma_n = P / h_1 = 50$ MPa. The critical point in the adhesive is placed at the interface adhesive-strap at the inner ends of the overlaps where the maximum peel stress is 1.5 times greater than the maximum shear stress. A completely different situation (Fig. 4) was observed in the case of the joint with tapered adherends where, in the critical point of the adhesive layer, the maximum shear stress is twice greater than the maximum peel stress.

Based on the results of NFEAs from table 1, one can observe that the maximum stress in adherends ($\sigma_{max,ad}$) was reduced 2.63 times and the maximum equivalent stress in adhesive was reduced 3.16 times in the case of tapered adherends comparatively with the variant with right adherends. In the case of the joint with right adherends the strength requirements (25) and (26) are not accomplished. On the contrary, the variant with tapered adherends is convenient, because $\chi = 0.133 < 1$ and $\sigma_{max,ad} = 91.1 \text{ MPa} \le \sigma_a$.

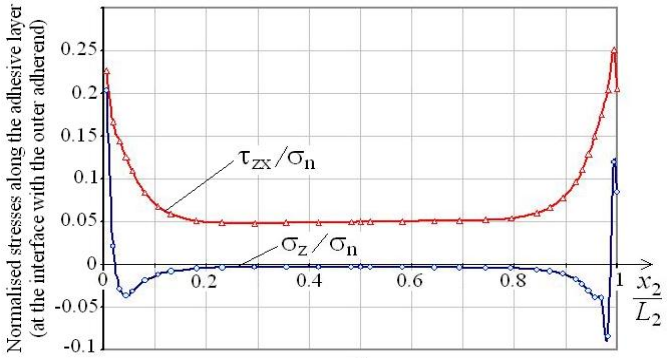
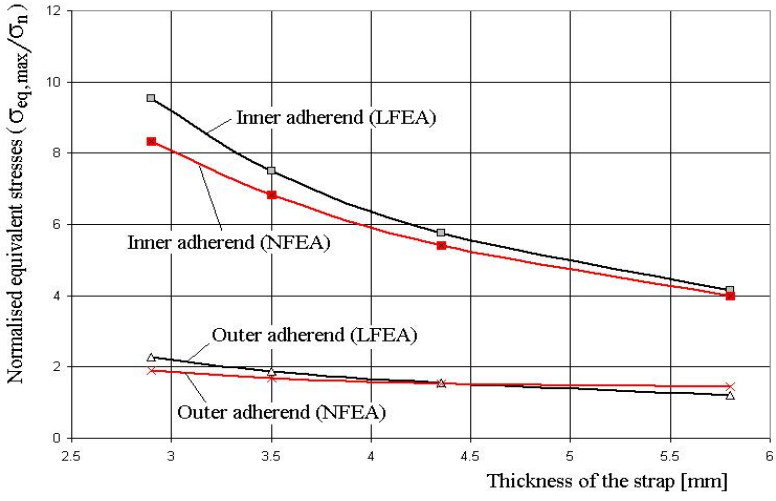


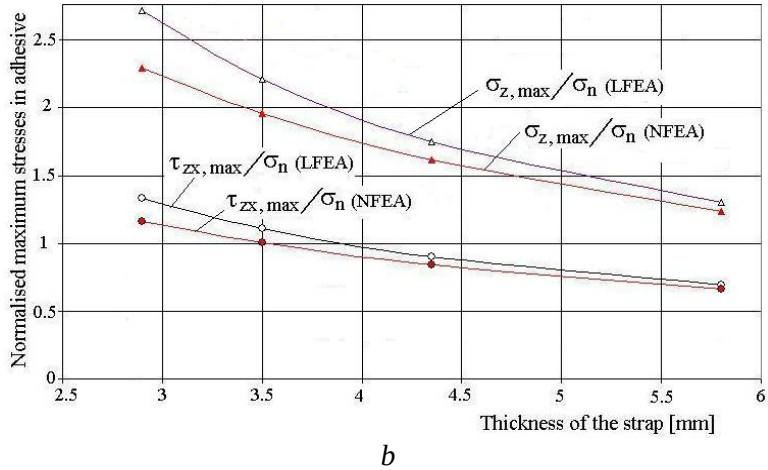
Fig.4 - Distribution of shear and peel stresses along the adhesive layer in the case of a single-strapped joint with tapered adherends, at the interface with the outer adherend

If the gap at the adherends ends is small ($L_3 < h/2$) significant discrepancies will be registered between the results, because the analytical formulas become inaccurate. Especially, the values of the maximum deflection, of the bending moment at the inner end of the overlap (M_i) and the maximum stresses in the adhesive are affected [7].

In order to emphasize the variation of geometrical nonlinearity when the strap thickness is increased, the case of a single-strapped joint with a small gap ($2L_3 = 0.4$ mm) between the adherends ends was considered as: $L_1 = 80$ mm, $L_2 = 20$ mm, h_1=2.9 mm, $h_3 = 2.9 \div 5.8$ mm, $h_a = 0.2$ mm and P = 145 MPa. The material properties were maintained as in the previous example. For comparison, linear elastic and nonlinear elastic finite element analyses were realised. It is noteworthy that the maximum stresses obtained by LFEAs are overestimated with 10÷13% comparatively to those given by NFEAs in the case when $h_1 = h_3 = 2.9$ mm, but a good concordance of results and a significant diminution of maximum stresses are obtained by increasing the thickness of the strap (Fig. 5,a and b). The major differences were observed between the maximum deflections (Fig. 6).



a



b

Fig. 5 - Influence of the strap thickness on the differences between the NFEAs and LFEAs results: a) maximum equivalent stresses in adherends, b) shear and peel stresses in adhesive

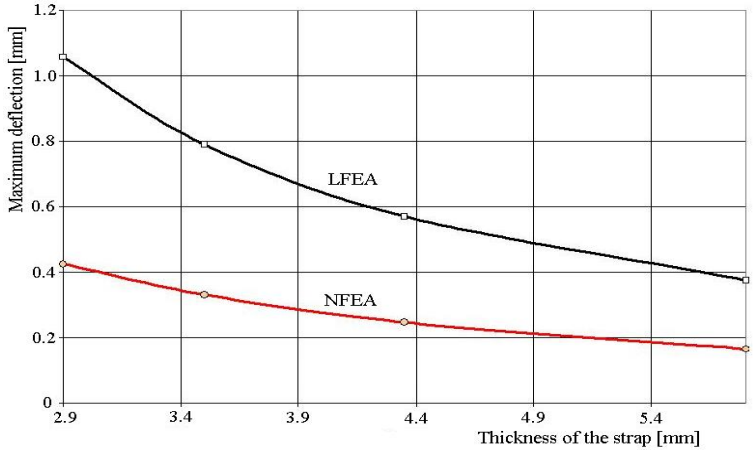


Fig. 6 - Differences between the maximum deflections obtained by NFEAs and by LFEAs

It is interesting to study the case when the gap between the adherends ends is filled with adhesive. On the other hand, in practice, this fact is inherent if the length of zone III is short. The case with P=145 N/mm, L_1=80 mm, L_2=20 mm, L_3=0.2 mm, h_1=2.9 mm, h_3=3.5 mm, h_a=0.2 mm was analysed both in the variants with unfilled and filled gap.

A great discrepancy between the behaviour of the two variants was found. The added adhesive has the desired effect, because a very important diminution of maximum peel and shear stresses in the basic adhesive layer is obtained, as is emphasized in figure 7.

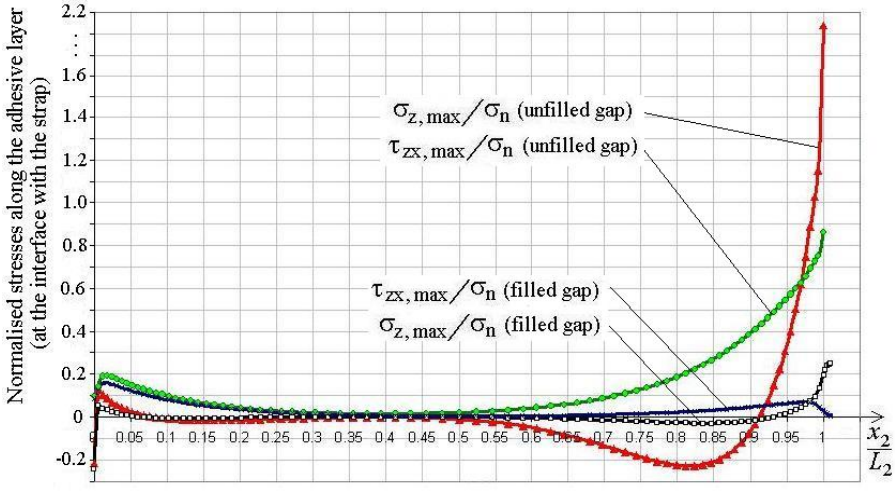


Fig. 7 - Variation of stresses in adhesive along the interface with the strap

The diagrams present the distribution of shear and peel stresses along the adhesive layer, at the interface with the strap, where was identified the critical point, at the inner end of the overlap. The stresses were normalised by dividing them with the nominal tensile stress in the outer adherends σ_n = 50 MPa. It is interesting that the maximum equivalent stress in the added adhesive is allowable, being of 36.9 MPa.

The adhesive added in the gap permits to obtain a spectacular reduction of stress concentration in adhesive as an effect of diminution of bending moment acting in the inner adherend of the joint.

4. CONCLUSIONS

The nonlinear analytical model is very useful for pre-dimensioning the balanced single-strapped adhesive bonded joints, but the obtained results are accurate especially if the overlaps and the gaps between the ends of the adherends are relatively large. A good agreement between analytical and nonlinear elastic finite element analysis results was observed. The linear elastic finite element analysis predicts correctly only the maximum equivalent stress in the outer adherend. Consequently, the behaviour of balanced or unbalanced single strapped joints in tension will be evaluated correctly if nonlinear analytical or numerical models will be used.

If the stress state in a single-strapped joint is evaluated then it is possible to apply appropriate strength criteria in order to establish the load capacity of the joint.

For design purposes it is worth to underline that a spectacular improvement of strength performance of single strapped-joints with small gaps between the adherends ends can be obtained by filling the gap with adhesive and by using straps thicker than the outer adherends.

REFERENCES

[1] D. Roach, K. Rackow, *Development and validation of bonded composite doubler repairs for commercial aircraft,* SANDIA Report SAND 2007- 4088, Sandia National Laboratories, Albuquerque, New Mexico, USA, July 2007.

[2] R. J. Clark, D. P. Romilly, *Linear coupled bending and extension of an unbalanced bonded repair,* Int. Journal of Solids and Structures, **44**, pp. 3156-3176, 2007

[3] C. N. Duong, *Design and validation of composite patch repairs to cracked metallic structures,* Composites, Part A, **40**, pp. 1320-1330, 2009.

[4] M. DAVIES, D. BOND, *Principles and practice of adhesive bonded structural joints and repairs*, Int. Journal of Adhesion and Adhesives, **19**, pp. 91-105, 1999

[5] L. J. HART-SMITH, *Designing to minimize peel stresses in adhesive bonded joints*, In "Delamination and debonding of materials", (Johnson W.S., editor), ASTM STP 876, pp. 238-266, 1985

[6] O. LUO, L. TONG, *Closed-form solution for nonlinear analysis of single-sided bonded composite patch repairs*, AIAA Journal, **45**, 12, pp. 2957-2965, 2007

[7] K. SHAHIN, F. TAHERI, *Analysis of deformations and stresses in balanced and unbalanced adhesively bonded single-strap joints*, Composite Structures, **81**, pp. 511-524, 2007

[8] M. SANDU, A. SANDU, D.M. CONSTANTINESCU, ST. SOROHAN, *The effect of geometry and material properties on the load capacity of single-strapped adhesive bonded joints*, Key Engineering Materials, **339**, pp. 89-96, Trans Tech Publications, Switzerland, 2009

[9] C. H. Wang, D. Erjavec, *Geometrically linear analysis of the thermal stresses in one-sided composite repairs*, Journal of Thermal Stresses, vol. **23**, pp. 833-851, 2000.

[10] D. R. Daverschot, A. Vlot, J. M. Woerden, *Thermal residual stresses in bonded repairs,* Applied Composite Materials, Kluwer Academic Publishers, **9**, pp 179-197, 2002

[11] * * * *Guide to the structural use of adhesives* (SETO), The Institution of Structural Engineers, London, 1999

[12] * * * *COSMOS/M – Finite Element System, User Guide*, Structural Research & Analysis Corporation, USA,1998